ChemComm

1D lanthanide halide crystals inserted into single-walled carbon nanotubes

Cigang Xu,[a] Jeremy Sloan,[ab] Gareth Brown,[ab] Sam Bailey,[a] V. Clifford Williams,[a] Steffi Friedrichs,[a] Karl S. Coleman,[a] Emmanuel Flahaut,[a] John L. Hutchison,[b] Rafal E. Dunin-Borkowski[b] and Malcolm L. H. Green*[a]

[a] *Wolfson Catalysis Centre (Carbon Nanotechnology Group), Inorganic Chemistry Laboratory, University of Oxford, South Parks Road, Oxford, UK OX1 3QR.. E-mail: malcolm.green@chem.ox.ac.uk*
[b] *Department of Materials, University of Oxford, Parks Road, Oxford, UK OX1 3PH*

Received (in Oxford, UK) 21st August 2000, Accepted 24th October 2000
First published as an Advance Article on the web 21st November 2000

1D crystals of lanthanide halides of the form $LnCl_3$ (Ln = La, Nd, Sm, Eu, Gd, Tb or Yb) have been inserted into single-walled carbon nanotubes (SWNTs) using the molten salt capillary filling method; *ca.* 20–40% of all the observed SWNTs were filled with melts in the range 650–910 °C with no observable damage to the carbon tubules; high resolution transmission electron microscopy (HRTEM) studies showed that the nanostructures of the encapsulated crystals varied with tubule diameter.

The unique physical properties of carbon nanotubes[1] have generated considerable interest and the expectation of new types of materials with useful practical applications. Theoretical studies[2–5] suggest that the introduction of foreign materials into their hollow cavities will have interesting effects both on the properties of the filling material and the filled nanotubes. Recently, the filling of SWNTs with Ru, silver metal and other species has been demonstrated.[6–10] Related work has shown that the doping of the interstices of SWNTs with vapour or liquid phase species, including alkali metals, bromine, or charged iodine chains, leads to a 10–100 fold decrease in their measured resistivities and to charge transfer behaviour detectable by Raman spectroscopy.[11,12] Lanthanide (or rare earth) ions have optical and magnetic properties that are particularly interesting when they are situated in a confined geometry. Additionally, as their spectral and dynamic properties alter when the reduced dimensions also affect the chemical and physical properties of the host, these species can act as a local probe for the chemistry and structure of the host material.[13] We present here preliminary results with respect to the incorporation and low-dimensional crystallisation properties of lanthanide halides within SWNTs.

Single-walled carbon nanotubes can be filled both by solution–deposition[6] or by capillarity[7–10] providing, in the latter case, that the filling medium has a surface tension in the range 100–200 mN m^{-1} and a melting temperature ideally below 900 °C.[7,14] The lanthanide halides $LnCl_3$ (Ln = Y, La, Pr, Nd, Gd or Dy) have surface tensions that fall below this threshold in the temperature range 820–950 °C.[15] In this study, we describe the filling properties of three of these halides (Ln = La, Nd and Gd) and four additional halides (Ln = Sm, Eu, Tb and Yb) for which surface tension data were unavailable (Table 1) but for which similar melting behaviour is assumed.

Samples of SWNTs were prepared by a high yield arc synthesis method.[16] The as-prepared SWNTs (*ca.* 30 mg) were intimately mixed with the anhydrous halides (*ca.* 70 mg) by grinding in an agate mortar and pestle under dry-box conditions. The samples were sealed under vacuum in a silica quartz ampoule that was then attached to the tip of a thermocouple and placed in a tube furnace. The temperature was slowly raised (3–5 °C min^{-1}) to a target temperature of *ca.* 10–50 °C above the melting point of the respective lanthanide chloride (Table 1), held at this temperature for 1 h and then furnace cooled to room temp. The specimens were characterised in a JEOL JEM-3000F FEGTEM operated at 300 kV (coefficient of spherical aberration (C_s) = 0.57; point resolution = 0.16 nm). Images were acquired digitally on a Gatan model 794 (1 k × 1 k) CCD camera, and the magnification was calibrated accurately using Si < 110 > lattice fringes. Energy dispersive X-ray microanalysis (EDX) was performed with a LINK 'ISIS' system using a 0.5 nm diameter electron probe.

All the lanthanide halides in Table 1 filled 20–40% of the observed SWNTs with continuous lanthanide halide single crystals. The HRTEM micrograph in Fig. 1(a) shows an example of $TbCl_3$ filling observed within a SWNT bundle. An enlargement of the tubule on the periphery of the bundle

Table 1 Surface tension data and synthesis conditions for lanthanide halides incorporated into SWNTs

SWNT filling material	Heating ramp rate/ °C min^{-1}	Melting temperature/°C	Target temperature/°C	Surface tension[a]/ mN m^{-1}
$LaCl_3$	3	860	910	109.407
$NdCl_3$	5	784	834	102.093
$SmCl_3$	5	686	706	—
$EuCl_3$	3	850	860	—
$GdCl_3$	3	609	659	91.7798
$TbCl_3$	5	588	638	—
$YbCl_3$	3	854	904	—

[a] Data not available for Ln = Sm, Eu, Tb or Yb.

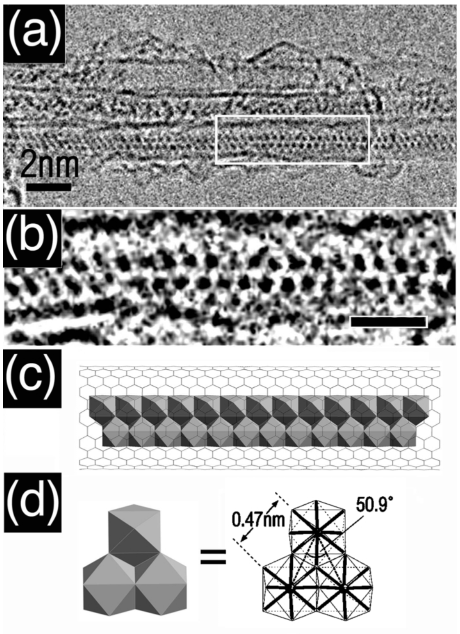

Fig. 1 (a) HRTEM image of $TbCl_3$ filling within a SWNT bundle. (b) Enlargement from boxed region in (a) showing a 'zigzag' arrangement of dark spots attributed to a 1D polyhedral chain of $TbCl_x$ polyhedra (scale bar = 1.6 nm). (c) Structural representation of a 1D polyhedral chain incorporated in a (12,12) SWNT. (d) Detail (left) and schematic depiction (right) of three polyhedra from the encapsulated chain shown in Fig. 1(c). The indicated dimensions in the schematic depiction are estimated from the lattice image [*i.e.* from (a) and (b)].

DOI: 10.1039/b006817i

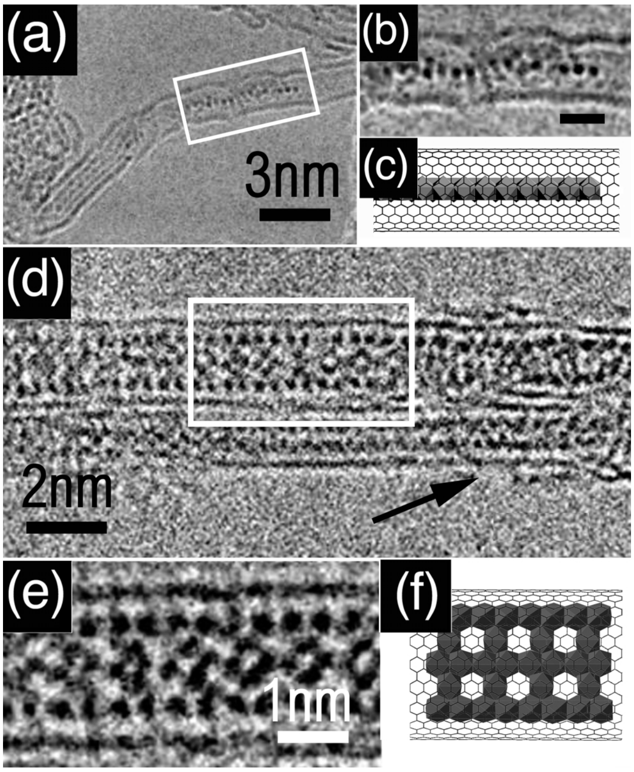

Fig. 2 (a) HRTEM micrograph showing a twisted 1D chain of $GdCl_3$ formed within a (10,10) SWNT. (b) Enlargement of boxed region from (a) showing a linear array of dark spots which terminates towards the right of the micrograph (scale bar = 1 nm). (c) Structural representation showing a 'top-down' view of (b) [*i.e.* similar to Fig. 1(c) but rotated 90°] about the SWNT axis). (d) Bundle consisting of one wide (*ca.* 2.5 nm) and one narrow (arrow = *ca.* 1.6 nm) SWNT both filled with $NdCl_3$. (e) Enlargement of the boxed region in (d) showing the unusual microstructure of the $NdCl_3$ filling. (f) Suggested structural model for (e).

[Fig. 1(b)] reveals that the crystal images as a 'zigzag' array of dark spots which we take to be a chain of $TbCl_x$ polyhedra. Most of the dark contrast in the 1D arrays must originate from the strongly scattering Tb^{3+} centres with the coordinating Cl^- ions being effectively invisible. Groups of three adjacent spots are arranged into nearly equilateral triangles of side *ca.* 0.47 nm. The bulk structure of $TbCl_3$ consists of $TbCl_9$ polyhedra arranged into a 3D hexagonal network (*i.e.* UCl_3-type[17,18]). Within the confines of the 1.6 nm diameter SWNT in Fig. 1(b), it is possible only to accommodate 1D polyhedral chains from the 3D structure, as shown in Fig. 1(c). The individual polyhedra within the chains are likely to be of reduced coordination owing to lattice terminations enforced by capillary confinement and the likeliest candidate structure is therefore a 1D network of edge-sharing $TbCl_6$ octahedra as depicted on the right of Fig. 1(c) (*cf.* $CdCl_2$[18]) and in detail in Fig. 1(d). We have recently reported a related reduction in coordination of 6 : 6 to 4 : 4 coordination for bilayer KI crystals incorporated into SWNTs.[19]

Fig. 2(a) shows a 1D chain of $GdCl_3$ incorporated into a 1.4 nm SWNT. The SWNT is bent into an 'elbow' and, on either side of the bend, the crystal images with different contrast suggesting a different orientation formed as a result of a twist induced by the bend. On the right of the bend, the crystal images as an apparently linear array of dark spots, as can be seen in the enlargement in Fig. 2(b). In this case we assume that the crystal has a similar structure to that depicted in Fig. 1(c) but that it is rotated 90° about the SWNT axis [*i.e.* relative to Fig. 1(c)] so that the polyhedral chain is viewed in 'top down' projection as depicted in Fig. 2(c). This crystal can also be seem to terminate within the SWNT capillary.

Fig. 2(d) shows a bundle of two SWNTs, one wide (*ca.* 2.5 nm) and the other narrow (*ca.* 1.6 nm), corresponding approximately to (12,12) and (20,20) SWNTs, respectively, both of which are continuously filled with crystalline $NdCl_3$. This crystal has an unusual microstructure as can be seen by the enlargement in Fig. 2(e). The encapsulated crystal consists of two linear 1D arrays of dark spots separated, in the middle, by a continuous series of groups of four dark spots arranged into diamonds. This microstructure cannot readily be reconciled with the bulk structure of $NdCl_3$,[18] but may instead correspond to the suggested arrangement in Fig. 2(f) in which 'diamond' arrays of $NdCl_x$ polyhedra formed along the centre of the SWNT are bounded by 1D arrays of $NdCl_x$ polyhedra formed along their walls. This arrangement is based using a similar interpretation as for Figs. 1(b) and 2(b), *i.e.* that each dark spot corresponds to a heavy Ln^{3+} centre within one or more $LnCl_x$ polyhedra viewed in projection.

In conclusion, we have demonstrated the first example of lanthanide halide insertion into SWNTs in high yield by a simple and reproducible method, and have also found that the diameter of the host SWNT profoundly influences the obtained structure of the filling material. The nature of these related crystallisation phenomena within SWNTs will be discussed more fully in a forthcoming publication. Experiments are also under way in our laboratory to understand the filling mechanism and to investigate the physical properties of these novel composites.

We acknowledge the Petroleum Research Fund, administered by the American Chemical Society (Grant No. 33765-AC5), the EPSRC (Grant Nos. GR/L59238 and GR/L22324) and Colebrand Ltd. for financial support. C. X. is grateful for a K. C. Wong Scholarship (University of Oxford), a Light Senior Scholarship (St. Catherine's College) and to the Henry Lester Trust. S. F. is indebted to BMBF and Fonds der Chemischen Industrie for additional financial support.

Notes and references

1 S. Iijima, *Nature*, 1991, **354**, 56.
2 K. Laasonen, W. Andreoni and M. Parrinello, *Science*, 1992, **58**, 1916.
3 J. W. Mintmire, B. I. Dunlap and C. T. White, *Phys. Rev. Lett.*, 1992, **68**, 631.
4 R. Saito, M. Fijita, G. Dresselhaus and M. S. Dresselhaus, *Mater. Sci. Eng.*, 1993, **19**, 185.
5 S. C. Tsang, Y. K. Chen, P. J. F. Harris and M. L. H. Green, *Nature*, 1994, **372**, 159.
6 J. Sloan, J. Hammer, M. Zweifka-Sibley and M. L. H. Green, *Chem. Commun.*, 1998, 347.
7 J. Sloan, D. M. Wright, H. G. Woo, S. Bailey, G. Brown, A. P. E. York, K. S. Coleman, J. L. Hutchison and M. L. H. Green, *Chem. Commun.*, 1999, 699.
8 C. H. Kiang, J. S. Choi, T. T. Tran and A. D. Bacher, *J. Phys. Chem. B*, 1999, **103**, 7449.
9 A. Govindaraj, B. C. Satishkumar, M. Nath and C. N. R. Rao, *Chem. Mater.*, 2000, **12**, 202.
10 X. Fan, E. C. Dickey, P. C. Eklund, K. A. Williams, L. Grigorian, R. Buczko, S. T. Pantelides and S. J. Pennycook, *Phys. Rev. Lett.*, 2000, **84**, 4621.
11 R. S. Lee, H. J. Kim, J. E. Fischer, A. Thess and R. E. Smalley, *Nature*, 1997, **388**, 255.
12 L. Grigorian, K. A. Williams, S. Fang, G. U. Sumanasekera, A. L. Loper, E. C. Dickey, S. J. Pennycook and P. C. Eklund, *Phys. Rev. Lett.*, 1998, **80**, 5560.
13 B. M. Tissue, *Chem. Mater.*, 1998, **10**, 2837.
14 T. W. Ebbesen, *J. Phys. Chem. Solids*, 1996, **57**, 951.
15 K. Igarashi, J. Mochinaga and S. Ueda, *Bull. Chem. Soc. Jpn.*, 1978, **51**, 1551.
16 C. Journet, W. K. Maser, P. Bernier, A. Loiseau, M. Lamy, M. L. de la Chapelle, S. Lefrant, P. Derniard and J. E. Fisher, *Nature*, 1997, **388**, 756.
17 H. Gunsilius, H. Borrmann, A. Simon and W. Urland, *Z. Naturforsch., Teil B*, 1988, **43**, 1023.
18 A. F. Wells, in *Structural Inorganic Chemistry*, Oxford University Press, Oxford, 5th edn., 1990, pp. 421–423.
19 J. Sloan, M. C. Novotny, S. R. Bailey, G. Brown, C. Xu, V. C.Williams, S. Friedrichs, E. Flahaut, R. L. Callendar, A. P. E. York, K. S. Coleman, M. L. H. Green, R. E. Dunin-Borkowski and J. L. Hutchison, *Chem. Phys. Lett.*, 2000, **329**, 61.